Journal of Scientific Exploration, Vol. 5, No. 2, pp. 163–190, 1991
Pergamon Press plc. Printed in the USA.

0892-3310/91 $3.00+.00

Ball Lightning and St. Elmo's Fire as Forms of Thunderstorm Activity

A. I. GRIGOR'EV, I. D. GRIGOR'EVA, and S. O. SHIRYAEVA
Yaroslavl University, Sovetskaya Str., 14, 150000, USSR

Abstract—The electrohydrodynamic theory of ball lightning and St. Elmo's fire is developed. Electrohydrodynamic instability of water droplets and films is basic for these phenomena and distinguishes them from corona.

1. Statistical Analysis

1. The author of one of the first studies on Ball Lightning (BL), W. Brand (1923), gave quite a complete list of properties of this natural phenomenon on the basis of 215 BL descriptions previously published by others. The list has been republished since then in a majority of books devoted to BL and to the physics of thunderstorms. It has also been used as a foundation for numerous attempts of theoretical and experimental modelling for this kind of lightning. Ball lightning was already presented as an electrodynamic effect and connected to St. Elmo's fire by Powell and Finkelstein. We will not dwell upon a detailed analysis of the list of BL properties, but just note that the division of BL into freely floating air and attached to conductors, introduced by Brand, as well as the proposed distinctions in the appearance of these two types, are supposed to be wrong.

To specify the foregoing discussion, we should note that, according to Brand (1923), BL attached to conductors are of white, dark blue, or light blue color and in most cases appear on the highest points of the conductors. In contrast to them, freely floating BL are of red color and are less bright than those attached to conductors. These two types of BL, according to Brand's assertions, can transfer to each other.

Brand's division of BL into two types is not trusted by the authors of the present article. More than 5000 unknown BL descriptions have been collected and analyzed by them and no traces of the existence of BL "attached to conductors" corresponding to Brand's concept (1923) have been found. It is natural to seek the reason for the contradiction arisen in that Brand interpreted as BL cases of another phenomenon of thunderstorm activity: St. Elmo's fire (SEF). To check the hypothesis, an investigation of the nature of SEF was carried out: descriptions of the phenomenon were collected by questioning the eyewitnesses who had observed it under natural conditions;

a theoretical model of the mechanism for SEF was built and checked experimentally (Grigor'ev & Sinkevich, 1984; Grigor'ev 1985 a & b; Grigor'ev & Grigor'eva, 1986). SEF turned out to be a rarer phenomenon than BL: only ≈200 of its descriptions were obtained. Some results of the statistical comparison of the collected testimonies of the SEF observations to 2100 descriptions of BL are presented in Figures 1–3, where the data referring to BL are marked by solid lines and the data referring to SEF by dashed lines. Figure 1 shows the probabilities of occurence of SEF and BL of a given color in the collected files of data. It is easy to see that in the great majority of descriptions, SEF are of white-dark blue-light blue color and BL are of red- orange-yellow color, all this coinciding with Brand's concept of attached to conductors and freely floating BL.

There is a strong correlation between observations of both SEF and BL and thunderstorm conditions. It has been found out that there is a statistically reliable correlational dependence between the frequency of BL observations in different months and the intensity of thunderstorm activity (the latter measured in the number of days with thunderstorms during each month). The obtained value of the coefficient of linear correlation between

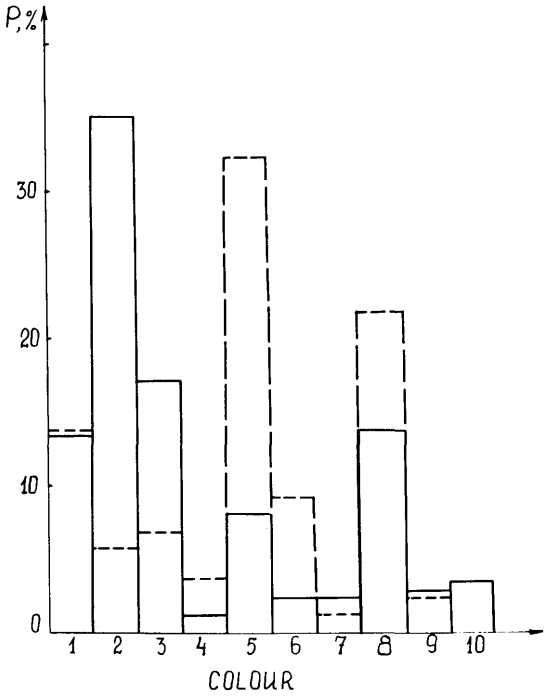

Fig. 1. Probabilities of BL and SEF occurence of a given color. The data referring to BL are drawn by solid lines, the data referring to SEF are drawn by dash lines. Numbers of colors 1—red, 2—orange, 3—yellow, 4—green, 5—light blue, 6—blue, 7—violet, 8—white, 9—rose, 10—lilac.

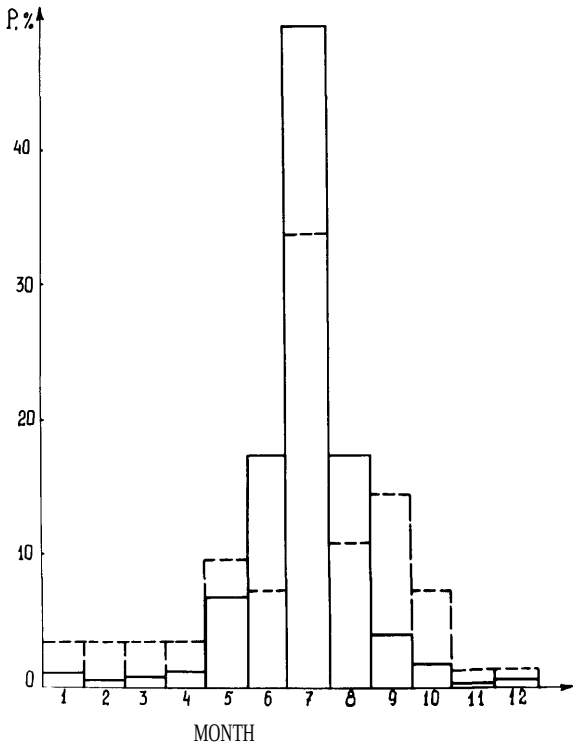

Fig. 2. Probabilities of BL and SEF occurence in different months of the year. The number of the month is shown on the horizontal axis. The data referring to BL are drawn by solid lines, the data referring to SEF by dash lines.

these events is ≈ 0.8 with a confidence level 0.98 (Grigor'ev, Grigor'eva, & Shiryaeva, 1988). Using the data from Matveev (1984) of the annual distribution of days with thunderstorms per month on the territory of the USSR and the data of the frequency of SEF observations in different months of the year, presented in Figure 2, it is easy to find the value of the coefficient of a linear correlation between the two events which is $\times 0.69$ with a confidence level of 0.99. The linear regression of the frequency of the monthly SEF observations x (as a percent of the total number) against the monthly recurrence of the days with thunderstorms y (also as a percent of the total number) has the form:

$$x = 8{,}3 + 1{,}2(y - 8{,}3)$$

Since there is a strong correlation between both SEF and BL and thunderstorm conditions, an unexperienced observer can easily mistake them. In addition, the characteristic linear dimensions of SEF $l \approx$ 10–15 cm are close enough to the statistically most probable diameter of BL which varies, according to different authors, from 7.5 to 14 cm (Grigor'ev et al., 1988). The

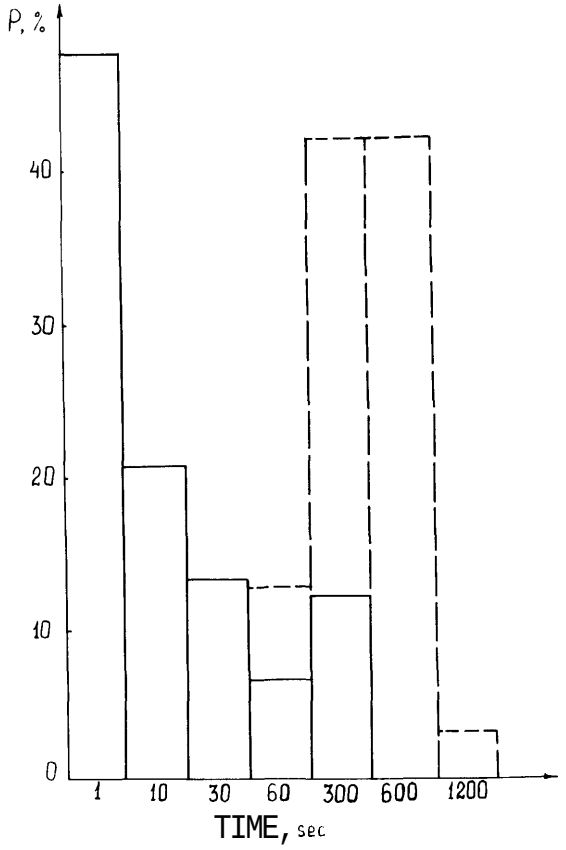

Fig. 3. Probabilities of BL and SEF occurence in the time interval shown as abscissa.

suggestion is also confirmed by the fact that 80% of the entire file of SEF observations refer to the time from 1 to 5 o'clock PM. This also accounts for Brand's assertion that BL attached to conductors (here interpreted as SEF) are brighter than those freely floating in air. According to the data (Grigor'ev et al., 1988), less than 4% of BL observations refer to the interval from 1 to 5 o'clock PM while the great majority of cases ($\approx$96%) were observed in daytime. It naturally makes the eyewitnesses report fainter luminescence.

The conditions of observation of SEF and BL are often similar to each other, and the distinction can be found only by a statistical analysis. The data on the probabilities of observations of SEF and BL under different geographical conditions are presented in Table 1. One can easily see that unlike BL, SEF occurs most often in the open country. A wind was reported in 69% of cases and a strong wind in 40%. Interestingly, the tonguelets of SEF luminescence do not sway even if the speed of the wind reaches 20 m/s.

Another property of SEF concerning the observation conditions is that they are always "attached" to an object: to the top of a mast, the edge of a

TABLE 1
Probabilities of observations of SEF and BL under different geographical conditions

Locality of Observation of the SEF or BL	SEF Observation Frequency in %	BL Observation Frequency in %
In the street of a settlment; inside the house	7.88	74.65
In the field	9.88	9.59
In the steppe	12.89	—
In the desert	6.59	—
In the mountains	21.98	2.27
In the forest	—	4.38
In the clouds; on a plane	10.89	5.13
In a sea, a lake, a river	24.89	4.03

bayonet, an aerial, the cross of a church, fingers of raised hands, etc. These objects are not always good conductors of electricity, but when **SEF** appear on insulators: wooden masts, oars, fingers, the objects are usually covered with drops or film of water. Humid air was reported in 72% of **SEF** descriptions: mist, rain, moist snow. In 52% of cases the surfaces were covered with drops or film of water.

The principle distinction in the descriptions of **SEF** and **BL** is their lifetime. The probabilities of existence of **SEF** and **BL** during an assigned period of time are presented in Figure **3.** It is easy to see that the **SEF** lifetime is much greater than the **BL** lifetime.

It is interesting to note that in 13% of **SEF** descriptions the eyewitnesses reported intensive radio noise accompanying **SEF.** With **BL** radio noises occur approximately in 1.3% of cases. This is evidently in correlation with the much shorter **BL** lifetime.

In 18% of descriptions **SEF** was accompanied by a specific sound such as a rustle or crackle. The smell of ozone from **SEF** was reported in 2% of cases. The corresponding probabilities for **BL** are $\approx$17% and 5% respectively.

2. The statistical comparison of the descriptions of **BL** and **SEF** has shown that the two forms of thunderstorm activity differ in the following important properties: ability to move, duration and autonomy of existence, characteristic color and intensity of luminescence, etc. On the other hand, **BL** and **SEF** have much in common: both are characterized by a strong correlation with thunderstorm conditions, their existence is accompanied by similar acoustic and olfactory effects, both are able to radiate electromagnetic waves in the radio range etc. All this makes Brand's error not accidental when he took **SEF** as a kind of **BL.** It means that by studying **SEF** we can approach solving the problem of **BL** origin and laws of existence. It is encouraging that not long ago **SEF** was universally considered a well-known phenomenon, the origin of which was associated with an intensive corona discharge from the conductors with small radii of surface curvature which arises during thunderstorms. The judgement was formed at the end of the last century on the basis of a purely visual similarity of **SEF** and a corona dis-

charge from a sharp metal point. Since then nobody has been specifically engaged in studying SEF and vivid contradictions in its interpretation and observation data have been left unnoticed. The contradictions, however, are quite obvious. SEF are widely known by intensive luminescence of a characteristic linear dimension up to ≈ 1 m, appearing along church spires and crosses, points of ship masts, i.e., at objects with characteristic radii of curvature not more than several centimeters. It means that the intensity of the electric field in the region of a characteristic linear dimension $\sim$ 1 m near such objects, ought to be greater than ≈ 30 kV/cm, but this value cannot be reached even inside a thunder cloud for so large a space [National Academy of Sciences (1986)]. So the results of Voitsekhovskii's experiments (Voitsekhovskii, 1982), in which he pointed out a significant role of water drops in SEF initiation, appeared quite unexpected. Then there arose a question of real properties of SEF observed under natural conditions as well as the problem of comparing real SEF to the phenomenon studied by Voitsekhovskii (1982), and to a corona discharge from a sharp metal point.

A thorough study of the collected descriptions has provided for distinguishing three forms of SEF which differ in both the conditions of initiation and physical mechanism for initiation: 1) Luminescence with the characteristic linear dimensions on the order of centimeters which arises on dry sharp metal objects, e.g., thorns of barbed wire barriers, bayonets of rifles, aerials—which can be naturally associated with an ordinary corona discharge from a sharp metal point (Figure 4). The descriptions of these cases were encountered in 10% of the entire file of descriptions. This form of SEF does not need any special comments and may be considered well-studied in connection with the investigation of a corona discharge from a sharp metal point. 2) Luminescence which arises during snowstorms and winter thunderstorms on any object during emission of snow- or hoarfrost-covered surfaces of

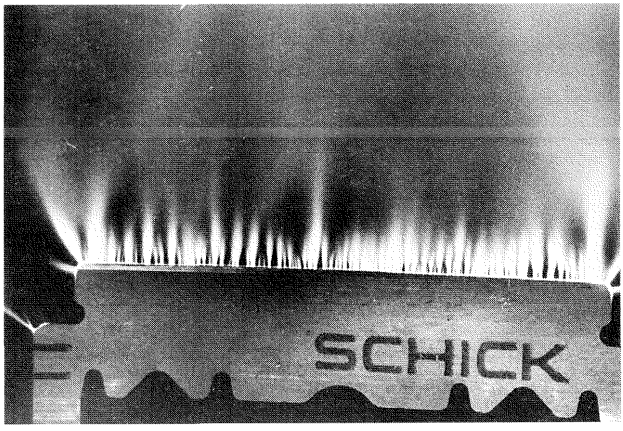

Fig. 4. A photograph of a corona discharge from the dry metal edge

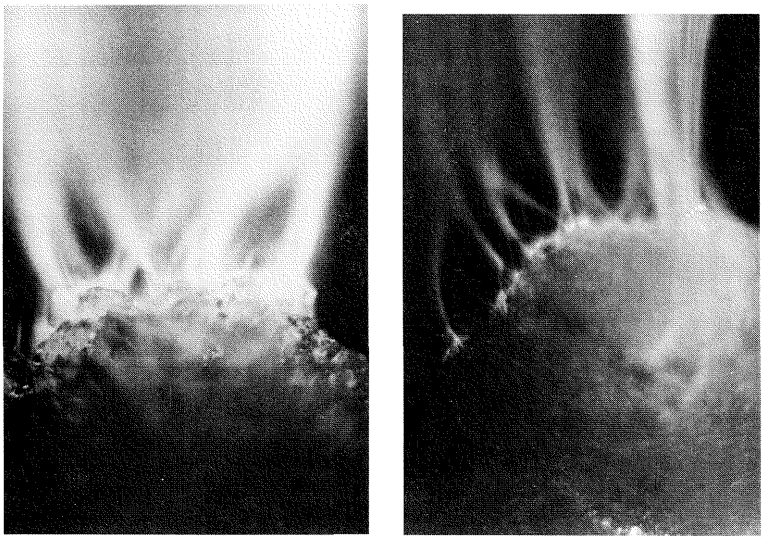

(a) (b)

Fig. 5(a) and **(b).** Emission on the moist snowball at the positive potential ≥ 10 kV applied. The paths of separate crystals are seen in the right part of the emission in Fig. **5b.**

heavily charged microcrystals of snow (Figure 5). This form of SEF was observed in 8% of descriptions. The characteristic linear dimension of the emission is ~ 10 cm. 3) Luminescence with the characteristic linear dimension up to 1 m arising under thunderstorm conditions on any object in humid air (in most cases when the surface is covered with drops or a water film), associated, according to Grigor'ev & Sunkevich (1984), Grigor'ev (1985 a & b), Grigor'ev and Grigor'eva (1988), with the instability of a water surface in an external electric field (Figures 6 & 7). This form of SEF was encountered in 82% of descriptions.

Of the above SEF forms, the third one is of the greatest interest from a theoretical point of view as it is the most complicated and less studied form of SEF. The second one is a special case of the third form in the sense of its physical mechanism for initiation of luminescence (Grigor'ev, 1985b). Therefore, we will restrict the foregoing theoretical examination by investigating the laws and conditions of initiation of the third form of SEF.

The third, most often encountered SEF form, in the authors' opinion, can be associated with the phenomenon of electrohydrodynamic instability of water drops and films on various objects in strong electric fields which are characteristic of thunderstorm conditions. In the final stage of development of the instability mentioned above, there occurs emission of highly disperse droplets carrying an electric charge which is a little larger than the critical one in the sense of the Rayleigh (1882) stability limit (Grigor'ev, 1988). The intensity of the electric field at the surface of these objects is high enough for initiation of a corona discharge self-sustained due to photoionization in the

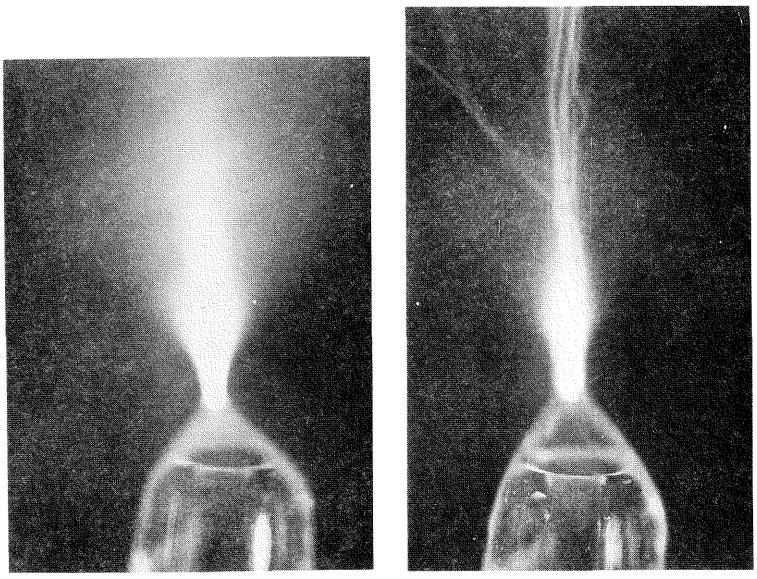

Fig 6(a). Diffuse (fan-shaped) emission at the discharge from the water meniscus on the capillary with the positive potential applied. (b) Emission at the electric discharge from the water meniscus of the radius 1 5 mm on the tip of the capillary with the positive potential 10 kV applied. The paths of separate droplets can be seen.

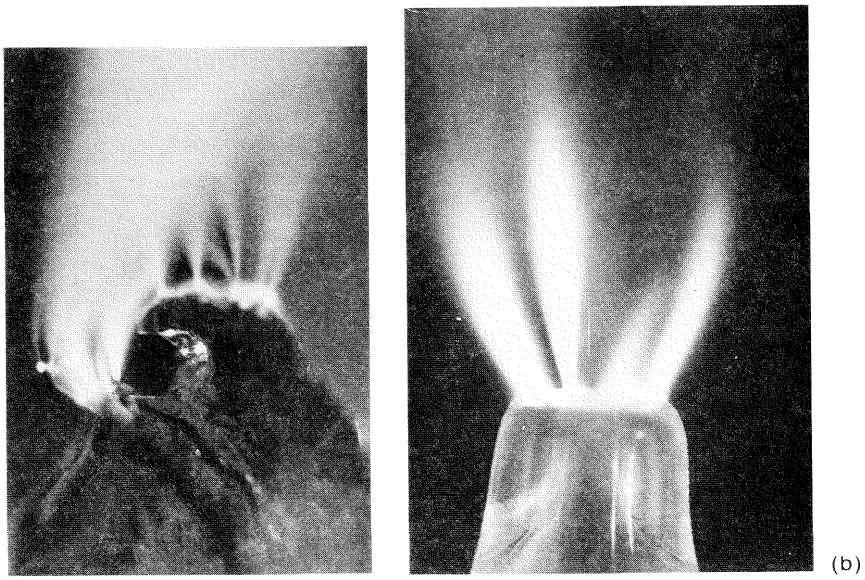

Fig 7(a) and (b). Emission at the discharge from the water film: on the surface of the melting ice (a) and on the section of the moist glass tube (b) with the positive potential applied.

immediate surroundings. It occurs as soon as an emitted droplet collides with a free electron or with a negatively charged ion (Grigor'ev & Sinkevich, 1984; Grigor'ev 1985a; Grigor'ev & Gigor'eva, 1986). The characteristic linear dimension of the bright region in the described model is determined by the mobility of the emitted droplets in the external field and is ≈ 100 cm. The critical intensity of the electric field at the object surface, covered with water drops or film, along which SEF may appear is ≈ 10 kV/cm, and such a field ought to exist only at the surface region with the characteristic linear dimension $\sim$ 1 cm.

We will now consider the discussion of the proposed mechanism for SEF initiation.

2. Calculation of the Parameters of Droplets

1. We calculated the parameters of droplets emitted by the surface of liquid under electrohydrodynamic instability in an external electric field. At electrohydrodynamic instability of the surface of a conducting liquid in an external electric field, some modes of capillary waves become unstable. At their superposition on the surface of a liquid, according to the mechanism proposed by Tonks (1935), from emitting protuberances. The critical condition for the development of such an instability on a flat surface of liquid (Tonks, 1935; Landau & Lifshitz, 1984) has the form:

$$\frac{E^2 a}{8\pi\sigma} \geq 1, \qquad (1)$$

where $a = \sqrt{\frac{\sigma}{\rho g}}$ is the capillary constant of liquid; ρ and a are the density and coefficient of surface tension of liquid; g is the acceleration of gravity; $\vec{E}$ is the strength of the external uniform electrostatic field perpendicular to the surface of liquid. Under condition (1) a capillary wave with the wave number $k = \frac{1}{2a}$ becomes unstable, and a system of protuberances appears on the surface of the liquid, with the amplitudes increasing with time. Due to the effect of polarization of liquid in the field E, the surface density of the charge on the protuberances will grow. With the increase of the amplitude of the protuberances (with the increase of the surface density of the charge), instability of capillary waves with the wave numbers larger than k will be generated on the protuberances Grigor'ev 1985C; Grigor'ev & Sinkevich, 1985). At the final stage of the described instability, emission of droplets will start from the tips of the emitting protuberances. The emitted droplets will have characteristic linear dimensions approximately one and a half orders of magnitude less than $2a$ and carry a charge a little larger than the maximum one in the sense of the Rayleigh stability limit (Brand, 1923; Grigor'ev & Shiryaeva, 1989). This circumstance seems not evident and we think it necessary to dwell on it.

2. If a spherical drop of the radius r and charge q tears from the tip of an isolated emitting protuberance and the full charge, the temperature and the volume of the liquid phase do not change, the change of free energy of the system in this act can be put as

$$\Delta F = 4\pi r^2\sigma + \frac{q^2}{2r} + \frac{E^2}{2}\left(\frac{r^3}{3} + C\right) + q\varphi, \qquad (2)$$

where C is a constant, whose value depends on the geometry of the system (the relief of the surface of the liquid and the electrodes producing the field). The first addend in equation (2) gives the energy of the forces of surface tension. The second gives the drop's own electrostatic energy. The third and the fourth addends are variations of the energy of external field $\vec{E}$, of the field of the induced charge in the drop and, the energy of interaction of the drop's own charge with the external field. If we fix the charge of the drop q we find the drop radius r at which A F will be extreme. Dividing this correlation by the first addend we obtain the extreme correlation between the drop characteristics and

$$\frac{\partial(\Delta F)}{\partial r} = 8\pi\sigma r - \frac{q^2}{2r^2} + \frac{E^2 r^2}{2} = 0;$$

$$W = \frac{q^2}{16\pi\sigma r^3} = 1 + \frac{\mathrm{E}^2 r}{16\pi\sigma} \equiv 1 + \mathcal{W} > 1. \qquad (3)$$

In this expression W is the Rayleigh parameter specifying stability of the drop with regard to its own charge. The drop is unstable at $W \geq 1$ (Rayleigh, 1882). The dimensionless magnitude W is the Taylor parameter with the accuracy to a constant and specifies stability of an uncharged drop in an external universal electric field (instability occurs at $W \gtrsim 0.05$). One can see from (3) that the extreme variation of free energy of the system at the emission of a charged droplet correlates with the emission of a drop which is unstable with regard to its own charge. Finding the second derivative of ΔF by r it is easy to see that this extreme is minimum.

As a result, emitted droplets are unstable referring to their own charge and disintegrate over time on the order of ten periods of oscillations of the fundamental mode of an uncharged drop of the same size, ejecting ~ 100 droplets which will be two orders of magnitude smaller and also unstable under the Rayleigh limit (Grigor'ev & Shiryaeva, 1988, 1989). The further process of successive cascade disintegrations of "daughter" droplets will go on until an elementary charge is left on the smallest daughter droplets. The characteristic dimensions of droplets at this stage of the process is ~ 1 nm (Grigor'ev, Zemskov, & Shiryaeva, 1988).

In each act, a disintegrating drop loses 30% of its initial charge and $\approx 0.5\%$ of its mass (Grigor'ev & Shiryaeva, 1988; Grigor'ev & Sinkevich, 1985). As a result, a system of stable droplets, which forms after the series of disintegrations is over, will be specified by the values of the Rayleigh parameter, ap-

proximately equal to half of the limit charge. We will not dwell on the discussion of these results since they are presented in detail in Grigor'ev and Shiryaeva (1988 & 1989) and Grigor'ev, Zemskov, and Shiryaeva (1988). We will just note that standardized per single interval functions of the distribution of the second and the third droplets according to their dimensions are presented in Figure 8a and Figure 8b correspondingly. The radii of the drops are made dimensionless regarding the radius of the initial drop, which tears off from the tip of the emitting protuberance. For water, according to what has been said in paragraph 1 of the given section, $r_0 \sim 0.03(2a) \approx 200$ mcm.

The reasoning given in this section of the paper is qualitative. One should take into account in a more strict theoretical examination, that the real shape of an emitted drop differs from spherical. One should also minimize variation of free energy of the system at the emission of one droplet according to two independent parameters: radius of the drop r, which is a characteristic of the change of the surface energy, and charge of the drop q which is a characteristic of the change of an electrostatic component of the free energy. The solution of the original problem given by Grigor'ev and Shiryaeva (1988 & 1989) is free from the drawbacks mentioned. However, since the results obtained above on the basis of simple and clear qualitative considerations are in conformity with the more accurate calculations of Grigor'ev and Shiryaeva (1988 & 1989) both qualitatively and quantitatively, we will not make numerical calculations according to the scheme. They are more correct but cumbersome.

3. An important role in the foregoing discussion is played by the magnitude of the intensity of the electric field near emitted droplets. Since, according to what has been said above, the value of the Rayleigh parameter for the rest of disintegrated droplets is ≈ 0.5, an expression for the strength of the field of the droplet's own charge E_q will be obtained after some identity transformations:

$$\frac{q^2}{16\pi\sigma r^3} = \frac{q^2}{R^4}\frac{R^4}{r^4}\frac{r}{16\pi\sigma} = \frac{1}{2}$$

$$\vec{E}_q = \frac{q}{R^2}\vec{n}_R = \left(\frac{r}{R}\right)^2 \sqrt{\frac{8\pi\sigma}{r}}\,\vec{n}_R. \qquad (4)$$

where R is the radial coordinate of the observation point; $\vec{n}_R$ is a single vector. Since the drop will polarize in the external field $\vec{E}_0$, a full expression for the intensity of the field near the drop will take the form:

$$\vec{E} = \sqrt{\frac{8\pi\sigma}{r}}\left(\frac{r}{R}\right)^2 \vec{n}_R + \left[1 - \left(\frac{r}{R}\right)^3\right]\vec{E}_0 + 3\left(\frac{r}{R}\right)^3(\vec{E}_0\vec{n}_R)\vec{n}_R \qquad (5)$$

3. Characteristic Linear Dimension of SEF Bright Region

1. As stated previously, the dimension of the SEF bright region seems to be connected with ignition of a corona discharge in the neighborhood of a

droplet emitted by the surface of liquid as well as of smaller droplets resulted from the Rayleigh disintegrations of the initial drops. For the critical strength of the field for ignition of a corona discharge E we take the one at which the effective coefficient of reproduction of electrons in an electron avalanche which develops in the field is greater than a unit. Since the entire process occurs in air under the atmospheric pressure, we take $E_* \approx 20$ kV/cm for a qualitative estimation (Lozanskii & Firsov, 1975).

It is easy to see from (5) that in the range of dimensions of droplets which is of interest ($r < 0.2$ mm), the field intensity in the surroundings of droplets will exceed E_*. Hence, there will exist, near the droplets, conditions necessary for initiation of a corona discharge sustained by photoionization. However, at least one free electron must be present in the immediate vicinity of the droplet before discharge can commence; but free electrons in the lower atmosphere are generated by natural radiation at a rate of ~ 10 cm^3 s^{-1} (Engle, 1955) and recombine in $\sim 10^{-8}$ s with neutral atoms and molecules to form negative ions. It is thus very unlikely that a droplet will collide with a free electron. However, in sufficiently strong electric field $E_+ > 90\ PV$/cm where P is pressure in mm of mercury (Lozanskii & Firsov, 1975; Engle, 1955), a negative ion is known to be destroyed and liberate an attached electron. The natural density of negative ions under natural conditions near the earth's surface is from 500 to 800 cm^{-3} (Engle, 1975), so that the probability that a droplet will collide with a negative ion, which subsequently breaks up and liberates an electron, is many orders of magnitude greater than for a free electron-droplet collision. (We will therefore neglect the free electron-droplet collisions in what follows.)

2. We assume for definiteness that the small droplet of the radius $r \approx 0.2$ mm is positively charged and that the intensity of the field at its surface is E ≈ 400 kV/cm. An electron located closer than a few radii from the center of the droplet will induce an avalanche of ~ 1000 electrons. If we repeat the estimates given in Ref. 18 for the number of secondary electrons generated by photoionization, we find that ~ 100–1000 secondary electrons will be produced within a radius of ~ 0.1 mm of the center. Under these conditions a self-sustaining discharge will form almost instantaneously.

For the above fields and radii, the charge on the small droplet will be $\sim 10^7 e$, where e is the electron charge. Therefore roughly 10^2 electron avalanches can proceed simultaneously so that the lifetime of the discharge around the droplet t_* will be two orders of magnitude greater than the growth time for a single avalanche, which is $\sim 10^{-7}$ s (Grigor'ev, 1985a); i.e., $r_* \sim 10^{-5}$ s.

Fig. 8(a) and (b) (See facing page). Normalized to unit interval functions of distribution according to the dimensions of the secondary (a) and the third (b) droplets which form during the Rayleigh disintegration of a heavily charged drop. Radii of the droplets made dimensionless on the radius of the initial drop r_0, which tears off from the tip of the emitting protrusion ($r_0 \sim 200$ mcm) are shown as abscissa.

It is easy to see that the total lifetime of the charged droplet is given by the sum where the first addend is the delay in discharge initiation t_0, determined by the probability that the droplet will collide with a negative ion, and the second, t_*, is the actual lifetime of the discharge itself. The linear diameter of the bright region of SEF will typically be comparable to the distance the daughter droplet travels in the external field E_0 before the self-sustained discharge near the droplet terminates.

The discharge delay time, i.e., the time interval from ejection of daughter droplet to collision with a negative ion, is given by

$$t_0 \approx \frac{1}{nVs}, \tag{6}$$

where n is the negative ion density, V is the velocity of the droplet when it collides with the ion, and s is the droplet-ion collision cross section. At atmospheric pressure, a negative ion will break up if it encounters a field of strength $E_+ \gtrsim 70$ kV/cm (Lozanskii & Firsov, 1975). Such fields are present within a radius of $R \lesssim \sqrt[4]{E_+^{-2}\,\pi 8\sigma r}$ of the center of the droplet; the cross section for nonelastic collisions between the droplet and a negative ion is therefore given by

$$s = E_+^{-1}\sqrt{8\pi^3\sigma r^3} \tag{7}$$

In dry air, the cross section for collisions between the droplet and a negative ion will be **3–4** times larger, since the field of the droplet will attract the negative ions over greater distances than the values determined by (7). However, in the humid air where SEF discharges are observed, each ion will be surrounded by **a** shell of water molecules and the resulting hydrated clusters will be very massive and immobile. We will therefore neglect the opportunity of attraction of the ions in the region with the field strengths $E \gtrsim 70$ kV/cm.

3. Thus, we assume that a small droplet of charge q and radius r **(4)** with zero initial velocity starts to move in an external field E_0 with acceleration

$$a = \frac{qE}{m} = \frac{3E_0}{4\pi\rho}\sqrt{\frac{8\pi\sigma}{r^3}}. \tag{8}$$

The expression for the droplet velocity during the time t_0 will be determined by the known expression:

$$t_0 = \frac{1}{\sqrt{nas}} = \sqrt{\frac{3E_0E_*}{nr^3}}$$

Then for the velocity of the droplet we find:

$$V = \frac{1}{2\pi}\sqrt{\frac{3E_0E_+}{nr^3}}$$

And the distance which the droplet travels during this time will be determined by the expression:

$$S = \frac{at_0^2}{2} = \frac{1}{2ns} = \frac{E_+}{\pi n\sqrt{8\pi\sigma r^3}} \tag{9}$$

We find from (6), (8), and (9) that for $r = 100$ mcm, $n = 800\ \text{cm}^{-3}$, $E_0 = 10\ \frac{\text{kV}}{\text{cm}}$, $S = 2$ cm, $a \approx 3 \cdot 10^5$ cm/s, $t_0 \approx 2.5$ ms, $V \approx 750$ cm/s. It is also easy to see that the characteristic distance the droplet travels up to nonelastic collision with an ion S and its velocity at this moment depends considerably on the radius of the drop $\sim r^{-3/2}$ and that already at $r = 0.01$ mm we will obtain $S \approx 60$ cm, $V \approx 2 \cdot 10^4$ cm/s.

In the above reasoning, evaporation of droplets has not been taken into account. Still, it is essential for droplets of micron dimensions. According to the results of the calculations of Zolotoi, Karpov, and Skyrat (1988), such droplets evaporate covering a distance ~ 1 cm. So $S \lesssim 1$ m seems a satisfactory estimate for the maximum characteristic linear dimension of the SEF bright region. One can see that under the conditions formulated above, a droplet will cover a distance negligible if compared to S, during the discharge time $t_* \sim 10^{-5}$ s. Consequently, the linear dimension of the bright region of SEF will be determined by the distance which is covered by the droplet during the time t_0.

It is seen from (9) that the characteristic linear dimension of the SEF bright region is in inverse ratio to the concentration of negatively charged ions in the SEF volume. Numerical estimation of the maximum value of the SEF characteristic linear dimension $S \lesssim 1$ m obtained above, holds only at $n = 800\ \text{cm}^{-3}$. One can naturally expect that at the initiation of SEF, the concentration of negative ions in their surroundings will increase. Indeed, according to what has been said above, intensive processes of photoionization of air occurs around the SEF volume (Lozanskii & Firsov, 1975). The ions which form in these photoionization acts will attach to neutral atoms to form negative ions. Finally, their concentration in the SEF volume will increase, and the characteristic linear dimension S will diminish to $\sim n^{-1}$. So the values, most often mentioned by the observers, correspond just to several centimeters (in 62% of observations $S \lesssim 5$ cm).

Under natural conditions, SEF having the characteristic linear dimension ~ 1 m are observed in thunderstorm weather at high, isolated objects such as church crosses, points of ship masts, etc. (Flammarion, 1873). In these cases a strong wind seems to blow out the surplus negative ions from the SEF volume, and the SEF flare occurs under the natural concentration of negative ions.

Indeed, at the speed of a storm wind ≈ 20 m/s and the discharge delay time in the droplet surroundings $t_0 \approx 2.5$ ms, the transverse to SEF displacement of the air is ≈ 5 cm. But there will be no noticeable blowing out of a charged droplet which moves along the field $\vec{E}_0$, since the Stokes force which carries the droplet away along the wind is one or two orders of magnitude less (depending on the radius) than the Coulomb force (at the values of

magnitudes accepted above). This accounts for the fact mentioned by the observers: SEF does not sway in the wind.

4. Electric Current Through SEF Radiation

1. If we consider that the frequency of the droplet emission from a single protuberance on the surface covered with a water film is on the order of the oscillation frequency of the fundamental mode of a tearing off drop

$$w = \sqrt{\frac{8\sigma}{\rho r^3}},$$

and that the tearing off drop carries a charge approximately equal to the limit according to Rayleigh

$$q \approx \sqrt{16\pi\sigma r^3},$$

it is easy to estimate the electric current flowing through the emitting protuberance:

$$t \approx qw = 8\sigma \sqrt{\frac{2\pi}{\rho}} \approx 0.4\ \mu\text{A}$$

The same currents, according to the order of magnitude, were reported in the experiments on studying electric discharge from a liquid electrode (Zeleny, 1914; English, 1948) as well as in Voitsekhovskii (1982). When there are several protuberances (N), the general current flowing through the discharge will increase N times.

2. As has been mentioned previously, SEF, accompanied by a sharp increase of the level of radio noises, often appear on parts of a plane: dielectric aerials—aerodynamic parts, sides of cabin lamps, points of propeller blades, making the flights very dangerous.

SEF appearance is associated with instability of the surface of a liquid in an electric field, under which emission of highly-dispersed, heavily-charged droplets occur from the tips of micro-protuberances, which form on the surface of the liquid, a corona discharge igniting around each of the droplets with some time of delay, sustained due to photoionization. According to Grigor'ev and Shiryaeva (1988 & 1989), at the instant when a drop is tearing off from the tip of an emitting protuberance, it has a shape similar to a protracted rotation elipsoid with the eccentricity ≈ 0.7. The fundamental mode of capillary waves of such a droplet becomes excited, and, since the droplet is charged, its oscillations will be accompanied by radiation of electromagnetic waves. If we consider, according to what has been said, that the size of daughter droplets can vary from $\sim$10 nm to 0.01 mm, depending on local physical conditions of SEF appearance, it is easy to find, within the frames of the model for radiation of an oscillating charged droplet, that the droplets will radiate electromagnetic waves in the range from 0.1 MHz to $1 \cdot 10^8$ Hz.

Thus the power of radiation of a single droplet of the size ~ 0.01 mm (up to complete expenditure of the initial energy) will be $\sim 10^{-16}$ W. It is obvious that the intensity of radio noises may be considerable when there is a considerable number of emitting protuberances.

When a corona discharge ignites in the neighborhood of charged droplets, another mechanism for radiation of electromagnetic waves, associated with the movement of electron avalanches, comes into force. The characteristic range of frequencies of this radiation with reference to the conditions of SEF is 1 MHz–$1 \cdot 10^8$ Hz (Olsen, 1983), its integral intensity being proportional to the current which flows through SEF.

5. Critical Intensity of an External Electric Field

1. According to what has been said, SEF appears at the surface of objects covered with a water film in the presence of rather a strong electric field in the medium. Then, at some critical value of the electric charge, capillary waves in the water film become unstable, and we can observe the picture described above.

According to criterion (3), the minimum surface density of the electric charge on the surface of the liquid κ, at which protuberances emitting charged and unstable under the Rayleigh limit droplets, will be determined by the correlation:

$$\kappa = \frac{1}{4\pi} \sqrt{\frac{8\pi\sigma}{a}} \tag{10}$$

The electric field intensity at which the charge determined by condition (10) appears on the surface of the liquid film, will depend on the surface curvature of the object covered with SEF. Thus, if the object has a shape similar to a cylinder, condition (10) for a water film will hold already at $E_0 \approx 10$ kV/cm. For a flat surface of a liquid the critical value of the external field is $E_0 \approx 25$ kV/cm. If we take into account that SEF most often appears at pointed objects (like masts and church crosses), the critical value of the external field may fall to $E_0 \approx 3$ kV/cm.

2. It should be noted that with the increase of E_0, visible luminescence of SEF will not necessarily increase. Thus at $E_0 \approx 100$ kV/cm, cluster shells of water molecules, covering negative ions, will disintegrate releasing ions (Grigor'ev & Sinkevich, 1984). The mobility of ions will grow, and they will be involved into the field of the droplet own charge from distances larger than $R = \{8\pi\sigma r^3 E_+^{-2}\}^{1/4}$. As a result, the section of the droplet-ion collision will increase and the characteristic dimension of SEF will diminish.

6. Comparison with Experimental Data

1. According to the model for the third SEF form proposed above, this phenomenon is accompanied with luminescence which forms by emission

emission results in the appearance of ~ 10 photoelectrons over a distance ~ 1 cm from the sharp point, in 10^{-7} s, according to the estimates of Lozanskii and Firsov (1975). These electrons, in the nonuniform electric field ≥ 10 kV/cm between the drop and the flat electrode, form avalanches which move toward the drop, i.e., a corona discharge will be sustained by photoionization.

4. If we return to SEF, we note that the emission associated with highly disperse charged droplets, which are ejected, can have a characteristic linear dimension ~ 1 m. The fan-shaped emission, on the other hand, has a characteristic dimension -- 1 cm, as has been mentioned before. These two manifestations of instability of water in an external electric field together can explain many aspects of SEF descriptions as well as Voitsekhovskii's experimental results (1982).

These experiments also furnish an explanation for an interesting fact: transition from the second stage of discharge to fan-shaped emission may occur even without an increase in the voltage across the discharge gap, if there is simply a hold for 2–3 min at a constant voltage. After this hold, a stable fan-shaped emission forms and is not interrupted by the ejection of droplets for tens of minutes. This fact may be evidence of, for example, a thermal activation of the transition from the second stage of the discharge to the fan-shaped emission: the Joule heating of the tip of the drop may intensify the field evaporation of H^+ ions and facilitate a transition to the fan-shaped emission.

5. It seems important to note that in Voitsekhovskii's (1982) experiments, luminescence of the SEF type occured when various grounded objects were brought into the cloud of unipolar charged drops. The drops settled down on the surface of the object, and an electric discharge commenced from them in the electric field of the cloud. By its visual characteristics it corresponded to the third form of the discharge from a liquid electrode described previously.

In developing the results of Voitsekhovskii's (1982) investigation, we carried out qualitative experiments in which water was sprayed through a nozzle of the radius 0.5 mm pneumatically in the apparatus pictured in Figure 9. A ring for induction charge of a copper plate 1 mm thick and 2 cm wide had a radius of 1.5 cm. A laboratory apparatus producing a potential difference up to 25 kV was used as a high-voltage source. One can find from elementary physical calculations that the charge which a drop acquires in an apparatus of the type presented in Figure 9 can be considerably greater than the maximum one according to the Rayleigh stability limit. It means that the drops which form at spraying a liquid the way it has been described, disintegrate spontaneously according to the above stated laws. This was proven in the course of experiments. In the dark room, a stream of sprayed water luminesced with light blue color over a distance of ≈ 5 cm beyond the induced ring. Luminescence of the same kind covered any object (e.g., an experimenter's hand) brought into the stream at a distance up to 0.5 m. This

Thus the power of radiation of a single droplet of the size ~ 0.01 mm (up to complete expenditure of the initial energy) will be $\sim 10^{-16}$ W. It is obvious that the intensity of radio noises may be considerable when there is a considerable number of emitting protuberances.

When a corona discharge ignites in the neighborhood of charged droplets, another mechanism for radiation of electromagnetic waves, associated with the movement of electron avalanches, comes into force. The characteristic range of frequencies of this radiation with reference to the conditions of SEF is 1 MHz–$1 \cdot 10^8$ Hz (Olsen, 1983), its integral intensity being proportional to the current which flows through SEF.

5. Critical Intensity of an External Electric Field

1. According to what has been said, SEF appears at the surface of objects covered with a water film in the presence of rather a strong electric field in the medium. Then, at some critical value of the electric charge, capillary waves in the water film become unstable, and we can observe the picture described above.

According to criterion (3), the minimum surface density of the electric charge on the surface of the liquid κ, at which protuberances emitting charged and unstable under the Rayleigh limit droplets, will be determined by the correlation:

$$\kappa = \frac{1}{4\pi}\sqrt{\frac{8\pi\sigma}{a}} \tag{10}$$

The electric field intensity at which the charge determined by condition (10) appears on the surface of the liquid film, will depend on the surface curvature of the object covered with SEF. Thus, if the object has a shape similar to a cylinder, condition (10) for a water film will hold already at $E_0 \approx 10$ kV/cm. For a flat surface of a liquid the critical value of the external field is $E_0 \approx 25$ kV/cm. If we take into account that SEF most often appears at pointed objects (like masts and church crosses), the critical value of the external field may fall to $E_0 \approx 3$ kV/cm.

2. It should be noted that with the increase of E_0, visible luminescence of SEF will not necessarily increase. Thus at $E_0 \approx 100$ kV/cm, cluster shells of water molecules, covering negative ions, will disintegrate releasing ions (Grigor'ev & Sinkevich, 1984). The mobility of ions will grow, and they will be involved into the field of the droplet own charge from distances larger than $R = \{8\pi\sigma r^3 E_+^{-2}\}^{1/4}$. As a result, the section of the droplet-ion collision will increase and the characteristic dimension of SEF will diminish.

6. Comparison with Experimental Data

1. According to the model for the third SEF form proposed above, this phenomenon is accompanied with luminescence which forms by emission

of highly disperse heavily charged droplets from the surface of water in an external electric field, with a corona discharge, self-sustained due to photoionization, igniting around the droplets. This model is somehow in opposition to the concepts which associate SEF with a corona discharge from a metal point, and which have been considered indisputable until the publication of the results of Voitsekhovskii's (1982) experiments. We have made an attempt to qualitatively check this model.

In the experiments, carried out by Zeleny's method, the high-voltage source was a laboratory apparatus producing a potential difference up to 25 kV. Our intention was to repeat the experiments of Zeleny (1914) and English (1948) to study qualitative features of fan-shaped luminescence at a discharge with reference to the model for SEF, and to compare the discharge from a drop to the discharge from a sharp metal point in this connection. Our experiments were carried out with drops 3 mm in diameter and a voltage -- 10 kV across an =3-cm discharge gap.

The general visually-observed picture of the discharge from the drop as the voltage across the discharge gap is increased can be summarized as follows. For a positive potential on the drop: (1) At the top of the drop a rapidly oscillating pointed protuberance appears and ejects a number of large charged droplets, which form a small pool on the flat upper electrode. In darkness, an extremely faint emission from the ejected droplets can be seen. The current is carried by the charges which are present on the drops. Photographs taken in daylight in this stage of discharge clearly reveal the two extreme positions reached by the tip of the drop during its oscillation. (2) The amplitude of oscillations and the emitted droplets become smaller. It is seen in darkness that emission from the ejected droplets is now accompanied by a diffuse component with a characteristic dimension $\sim$ 1 cm, "attached" to the protuberance, on the drop tip. The current is carried both by charges on the droplets and by ions. Photographs, taken in darkness, reveal the paths traced out by the emitting droplets which are ejected, and also a diffuse glow near the tip (Figure 6). (3) With further increase of voltage, oscillations of the protuberance and emission of droplets terminate completely. The upper electrode remains dry. At the tip of the drop in darkness, we can clearly see an intense fan-shaped emission which fills the entire discharge gap (Figure 6a). The current is carried by ions. (4) Extremely intense oscillations appear, involving the entire drop. The field tears large "pieces" of water from the drop. The general appearance of the discharge roughly corresponds to the second stage, but now the tracks of the ejected droplets are far wider and fainter.

When a negative potential is applied to the drop, we observed the same stages, but diffuse emission is far weaker, its characteristic dimension does not exceed 2 mm, and the emitted droplets do not glow. It is difficult to draw sharp boundaries between the various stages in terms of the voltage across the discharge gap, since these stages are rather arbitrary and are determined by a large number of external parameters: the size of the drop, the electrical

conductivity of the liquid and the external medium, the distance between the electrodes, the surface tension and viscosity of the liquid, and the emission properties of the liquid and of the flat electrode.

For both polarities, the discharge from the drop is, in its third stage, visually very similar to a corona discharge from a sharp metal point under the same external conditions (cf., e.g., the positive corona from the sharp metal point in Figure 4 to fan-shaped emission in Figure 6a). However, an attempt to identify their physical mechanisms on this basis will probably lead to incorrect results. This can be seen from the experiments carried out be English (1948). He studied, in particular, the discharge from a negative drop for various pressures in the medium. In contrast to the properties of a corona discharge, the voltage at which the discharge commences from the drop is absolutely independent of the pressure. English concludes that the discharge in the case of a negative potential on the drop is not a corona, despite the outward similarity. His conclusions seem convincing in view of the small value of the second Townsend coefficient for water (the work function of water is ≈ 6.1 eV). In our opinion however, English overlooked the possibility for an ion emission from the drop. This form of discharge from the drop may be classified as a corona discharge if we take into account the possibility of field evaporation of OH^- ions and negative impurity ions (Zolotoi, Karpov, & Skyrat, 1988) from the tip of the sharp liquid point. Destruction of these ions in the strong field near the sharp point (>70 kV/cm) gives rise to the "seed" electrons required for a negative corona. In this case it is easy to explain the independence of the discharge ignition voltage from the pressure in the medium. We also see the explanation for the curious tendency toward the formation, in the third stage of the discharge, of several microscopic sharp points which move over the negatively charged drop, with tiny tongues of emission ~ 1 mm in size attached to their tips. Specifically, sharp crests appear on the high-index capillary waves which are growing in the strong external field in the nonlinear stage, and an emission of negative ions becomes possible. These ions can then be destroyed, with the result that electrons are liberated and form electron avalanches. This model suggests that the discharge from a drop with a positive potential in the stage of the fan-shaped emission may also be a consequence of H^+ ions which have been evaporated by the field from the tip of a sharp point on the drop.

Indeed, field evaporation of ions from a sharp liquid point occurs at fields $\sim 10^8$ V/cm (Zolotoi, Karpov, & Skyrat, 1988), which arise at a voltage of only $5 \cdot 10^3$ V and at a radius of curvature $\sim 10^{-5}$ cm for the tip of a sharp point. Since the mean free path of an ion with respect to collisions with neutral molecules in air at atmospheric pressure is $\sim 10^{-5}$ cm, the energy acquired by a H^+ ion in the field is $\sim 10^3$ eV. A proton with this energy can cause the ionization and excitation of molecules over a distance $\sim 10^{-4}$ cm from the sharp point in air at atmospheric pressure. As a result, at a current $\sim 10^{-6}$ A (which flows in this stage through a drop ≈ 1 mm in diameter) $\sim 10^{15}$ excited molecules will form per second near the sharp point; their

emission results in the appearance of ~ 10 photoelectrons over a distance ~ 1 cm from the sharp point, in 10^{-7} s, according to the estimates of Lozanskii and Firsov (1975). These electrons, in the nonuniform electric field $\geq 10\,kV/cm$ between the drop and the flat electrode, form avalanches which move toward the drop, i.e., a corona discharge will be sustained by photoionization.

4. If we return to SEF, we note that the emission associated with highly disperse charged droplets, which are ejected, can have a characteristic linear dimension ~ 1 m. The fan-shaped emission, on the other hand, has a characteristic dimension -- 1 cm, as has been mentioned before. These two manifestations of instability of water in an external electric field together can explain many aspects of SEF descriptions as well as Voitsekhovskii's experimental results (1982).

These experiments also furnish an explanation for an interesting fact: transition from the second stage of discharge to fan-shaped emission may occur even without an increase in the voltage across the discharge gap, if there is simply a hold for 2–3 min at a constant voltage. After this hold, a stable fan-shaped emission forms and is not interrupted by the ejection of droplets for tens of minutes. This fact may be evidence of, for example, a thermal activation of the transition from the second stage of the discharge to the fan-shaped emission: the Joule heating of the tip of the drop may intensify the field evaporation of H^+ ions and facilitate a transition to the fan-shaped emission.

5. It seems important to note that in Voitsekhovskii's (1982) experiments, luminescence of the SEF type occured when various grounded objects were brought into the cloud of unipolar charged drops. The drops settled down on the surface of the object, and an electric discharge commenced from them in the electric field of the cloud. By its visual characteristics it corresponded to the third form of the discharge from a liquid electrode described previously.

In developing the results of Voitsekhovskii's (1982) investigation, we carried out qualitative experiments in which water was sprayed through a nozzle of the radius 0.5 mm pneumatically in the apparatus pictured in Figure 9. A ring for induction charge of a copper plate 1 mm thick and 2 cm wide had a radius of 1.5 cm. A laboratory apparatus producing a potential difference up to 25 kV was used as a high-voltage source. One can find from elementary physical calculations that the charge which a drop acquires in an apparatus of the type presented in Figure 9 can be considerably greater than the maximum one according to the Rayleigh stability limit. It means that the drops which form at spraying a liquid the way it has been described, disintegrate spontaneously according to the above stated laws. This was proven in the course of experiments. In the dark room, a stream of sprayed water luminesced with light blue color over a distance of ≈ 5 cm beyond the induced ring. Luminescence of the same kind covered any object (e.g., an experimenter's hand) brought into the stream at a distance up to 0.5 m. This

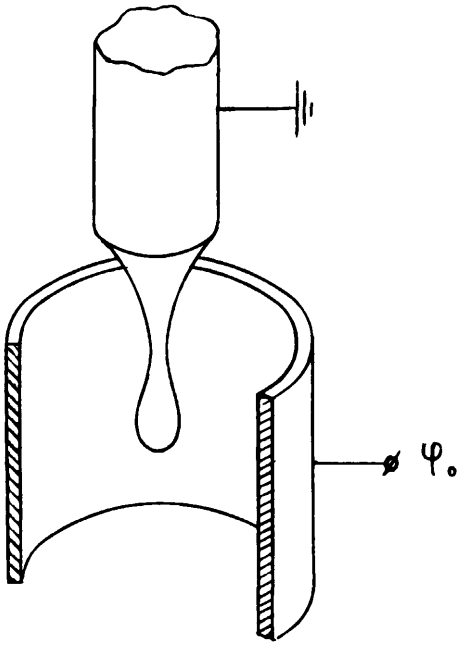

Fig. 9. Scheme of the apparatus for inductive charging of drops during the pneumatic spray of water.

directly points to the Rayleigh disintegrations of droplets which occur both right outside the induced ring and at a certain distance from it.

7. The Second Form of SEF: Emission at Electric Discharge From the Surface of Snow and Ice

1. We have already noted that about 8% of SEF descriptions appeared in winter during snowfalls and snowstorms near snow-covered surfaces. We have accordingly carried out some experiments, described below, whose purpose was to determine qualitative features of a corona discharge from the surface of snow and ice and to see if it is possible to identify it with SEF. As in paragraph 6, in these experiments, a high-voltage source was a laboratory apparatus which produced a potential difference up to 25 kV. A non-uniform electric field was produced between a flat copper upper electrode and the surface of snow or ice. The protuberances had a characteristic linear dimension $\sim$ 1 cm. Emission which occured upon the onset of the corona discharge from the surface of snow or ice was photographed in darkness by a Zenit-E camera with a Gelius-44 objective on a film with a speed of 350 (with the iris completely open), at a distance $\approx$ 15 cm.

2. We must report at the very beginning, that for either sign of the potential applied to the ice electrode, a diffuse discharge is absent at any values of

the intensity of the electric field achieved in the experiment, if the electrode is dry and smooth, without water drops or hoarfrost. When, as a result of heat exchange with the surrounding medium, the electrode gets warm, a corona discharge begins as soon as moisture appears on it. The discharge starts from a water bulge which forms on one of the highest points of the electrode and has a shape of a sharp protuberance with a characteristic linear dimension $\sim$ 1 mm. The width of the moist layer does not exceed 0.1 mm and the water film is practically invisible.

The appearance and size of the sharp protuberances with a corona discharge completely correspond to the description and sketch given by Grigor'ev (1985a), which deals with luminescence on objects brought into a cloud of charged droplets. Apparently, some streams, directed to the discharge location, form under the influence of forces in the external field, which provide formation of the discharge protuberance.

The intensity of the discharge luminescence right after its ignition is small, and the discharge is unstable: it dies out in $\approx$1–3 s, as the reserve of moisture near the discharge protuberance, which has the initial characteristic dimension of $\sim$1 mm, shrinks rapidly, disappearing completely in 1–3 s. The discharge also dies out. After about a minute, it reignites and flares intensively and smoothly. As the reserve of moisture is replenished during the melting of the electrode in some minutes, the discharge becomes more intensive. In addition, several discharge protuberances appear in the neighboring points, with emission on their tips. When the moisture is ladled from the ice electrode, the discharge dies out, and it does not reignite until water reappears on the electrode due to heat exchange with the surrounding medium. When the ice electrode is cold enough, there is only one discharge protuberance, since there is little water on its surface. In this case it is possible to stop the discharge by bringing a sheet of dry paper into the discharge gap (without touching the electrodes) for 1–2 s. The discharge protuberance disappears under the influence of gravity, and we have to wait for $\sim$1 min for it to reignite until a new discharge protuberance forms.

A discharge from a dry ice electrode covered with hoarfrost is ignited easily but the emission is faint and has an obvious banded structure which indicates that it occurs due to the emission of charged microscopic hoarfrost crystals. When the surface of the electrode melts slightly, the adhesion forces between the microscopic crystals intensify, the crystals losing their sharp edges with melting, and the discharge dies out. In $\approx$1–3 minutes it is reignited as the voltage across the discharge gap is increased. In addition, we observe in this case a previously absent diffuse component of the emission. This component pulsates with a period of 1–5 s and intensifies with the increase of moisture on the electrode surface. After the hoarfrost crystals melt completely, the discharge dies out and does not reignite until the surface of the ice electrode is covered with a water film.

If the electrode has a shape of an angle $\lesssim$ 30 with the radius of vertex curvature $\sim$ 1 mm, the height $\approx$ 3 cm, a corona discharge does not flare

even on the vertex, though the field intensity at the vertex reaches ~100 kV/cm. The apparent reason is that the entire moisture, resulting from the ice melting, pours down to the field of gravity. A stable discharge ignites at the height of the ice protuberance, having the shape of the angle, which does not exceed 1 cm.

The discharge picture in this case is apparently connected with a low conductivity of ice which is not less than two orders of magnitude lower than that of water (Griffiths & Latham, 1974). Interestingly, the conditions of the discharge ignition depend on how the potential is applied to the ice electrode: a wire can be soldered into the electrode or the potential can be applied to the electrode surface. In the latter case, a corona discharge is ignited at a lower voltage and has greater intensity. This fact is in conformity with the conclusion of Griffiths & Latham (1974) that for a discharge from an ice electrode the surface conductivity of ice is more essential than the conductivity of its volume. It is also proved by the fact that when we have a prolonged discharge from an ice electrode, some paths are melted on its surface, which lead to the discharge location from the place of the potential apply. This is apparently due to the Joule heat radiation during the current flow. Such a melting of paths occurs both when the potential is applied to the surface of the ice electrode and when the wire is soldered inside it. In the latter case, the paths are melted from the location of the contact between the metal conductor and the ice to the nearest point of the surface and lead along to the discharge location.

3. At a discharge from the surface of a dry snow electrode, a faint banded emission, the same as a discharge from a dry ice electrode covered with hoarfrost, easily arises. It also changes in appearance when heated and the electrode melts.

It is interesting to note, that at a sufficiently large potential difference when a positive potential is applied to an electrode of dry and porous snow, the field will occasionally pull off pieces of snow $\approx$ 3 mm in diameter from the electrode. In the field, these pieces of snow are accelerated to a high velocity and, when they collide with the copper upper electrode, they fly apart in glowing sparks over a distance up to 30 cm. This reveals a positive electric charge on separate snow crystals which is large enough that a self-sustaining by photoionization corona discharge can ignite near the crystal, as in the third model for SEF during the emission of positively charged droplets.

4. The dependence of the emission volume and intensity on the sign of the potential applied to an ice (snow) electrode is the same as for a discharge from a water drop: when a positive potential is applied, the appearing emission is rather intense and fills the entire discharge gap $\approx$ 3 cm; when a negative potential is applied, the emission intensity is weaker, and its characteristic linear dimension does not exceed $\approx$3–4 mm.

Luminescence of a positive discharge from ice and snow electrodes photographed with the exposure 4 s is given in Figure 7 and Figure 5 correspondingly. A negative discharge from ice and snow electrodes photographed with

the exposure 30 s is given in Figure 10 and Figure 11. As in the case of a discharge from a water drop, the emission tonguelets of a negative discharge on ice and snow electrodes are more mobile than those of a positive discharge. On a snow electrode, the tonguelets are more numerous and mobile than on an ice electrode. This apparently results from the heterogeneous surface of the snow electrode as well as from the specific way the fluid is supplied to the location of the discharge flare along the snow pores.

On an ice electrode, the tonguelets of a negative discharge flare rather evenly: they do not die out but Just move along the ice surface.

On a snow electrode, the emission tonguelets of a negative discharge Rare up and last about 5–10 s, then disappear and flare up again at a neighboring point.

There is a difference in the shape of emission of a positive and negative discharges which is seen in the photographs and which was mentioned in Zeleny's (1914) works devoted to a discharge from liquid electrodes.

5. The emission of a positive corona from moist ice (Figure 7) is similar in appearance to the descriptions of the fan-shaped emission which arises during a discharge from a water drop. It differs from that emission, however, in that as the voltage across the discharge gap is changed, we do not observe changes in the succession of the various stages of the discharge which are characteristic for discharges from water drops.

The only change at the emission of a positive corona from moist ice is in the intensity of the emission with the increase of the voltage applied. There is no change in the succession of the stages of the discharge. The emission is diffuse at any values of the field. The apparent reason is a deficiency of moisture at the surface of the ice electrode. This moisture is supplied to the discharge protuberance (located, as a rule, on the highest point of the elec-

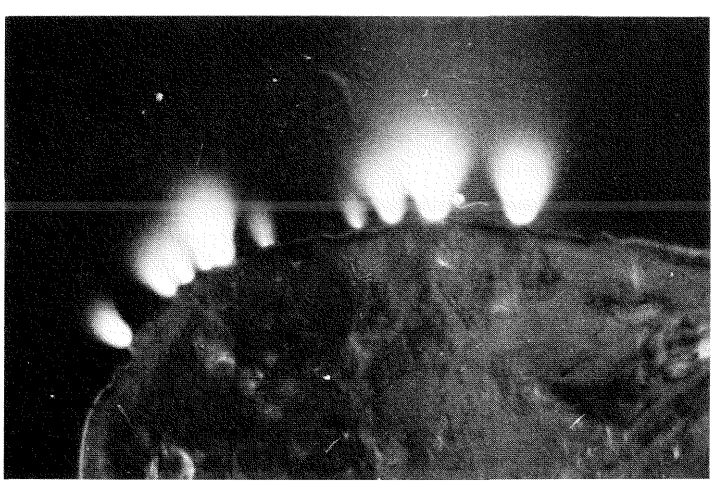

Fig. 10. Emission at the moist ice electrode with the negative potential applied.

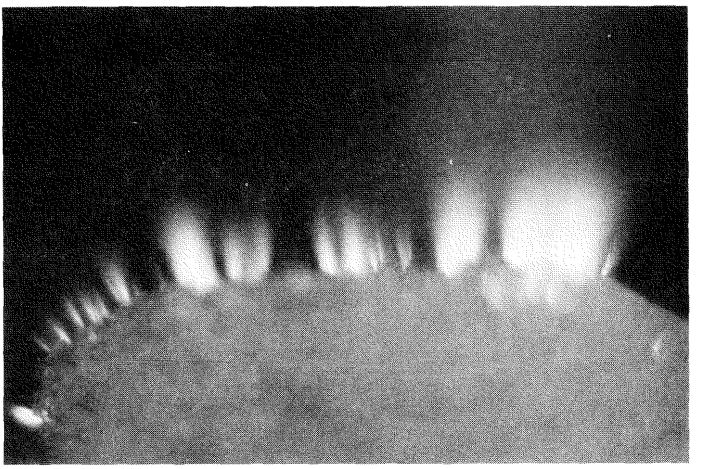

Fig. 11. Emission at the moist snow electrode with the negative potential applied.

trode) by fluxes which are set up in a water film, and their intensity is not high enough to lead to the formation of water drops at the tip of the discharge protuberance. However, we can exclude an opportunity of emission of small droplets on the bare fact that we cannot observe them with the naked eye. Formation of droplets $\lesssim 0.01$ mm in diameter at the tip of the discharge protuberance is quite possible.

6. The emission of a positive discharge from a melted snow electrode (Figure 5) is similar to the emission of a positive discharge from an ice electrode. No change in the succession of the various stages of the discharge can be observed as the voltage across the discharge gap is increased, and with the change of voltage applied, only the intensity of the diffuse emission changes. As for the discharge emission from a snow electrode, it has a number of peculiarities which can not be observed at the discharges from either ice or liquid electrodes.

The emission of a discharge from a snowball is pulsating. About ten emission tonguelets exist simultaneously, each lasting from 10 to 20 s; after a tonguelet disappears, it flares up again 1–2 s later at the same point or at a neighboring point. The emission is uneven as at the discharge from an ice electrode. It consists of separate bands and lines which can be clearly seen against the general background of the diffuse emission (Fig. 5 in its right part). This banded structure of the positive discharge is probably associated with the emission of microcrystals of snow. The pulsations probably occur due to the specific way moisture is supplied to the discharge location through micropores in the snow electrode. It is the diffuse emission that has these pulsations. The banded emission, which is supposed to be associated with the emission of snow microcrystals, appears and disappears, according to what has been said above, without any clear dependence on the magnitude of

the voltage across the discharge gap or the moisture content on the snow electrode. With the increase of moisture content, the pulsations become less noticeable. The intensity of the corona emission also increases with the increase of moisture content in the snow electrode.

It should be pointed out that the banded discharge emission from the snow electrode differs in appearance from the emission at the discharge from a water drop when it emits highly disperse droplets. First, one cannot notice banded emission at the discharge from a drop. The emission of the ejected droplets has a yellow tinge against the violet blue background of the diffuse luminescence. When a charged droplet is ejected by the discharge protuberance on the tip of a water meniscus, the intensity of the diffuse emission falls on tenths of a second. The banded discharge emission from a snow electrode has the same color as the diffuse emission, is present simultaneously and independently. The apparent reason is that snow microcrystals are emitted not be the discharge protuberances but directly by the surface of the snow electrode, i.e., by small roughnesses of its surface. In addition, it is quite probable that the dimensions of the emitted snow microcrystals are much less than the dimensions of the droplets ejected by the discharge protuberances on the drops.

The magnitude of the charge on microcrystals may be much greater than it is on the drop, since it is not restricted by the conditions of the Rayleigh (1882) limits. The maximum value of a crystal charge can be estimated by the order of magnitude, proceeding from general physical considerations. Indeed, the electric forces associated with the presence of a charge on the crystal can destroy a crystal of a characteristic linear dimension I and charge q, when the energy of the charge field $U_1 \approx \frac{q^2}{2l}$ exceeds the elastic energy of the crystal

$$U_1 \approx k l^3$$

Here k is the Young modulus for ice. When we compare the two expressions, we can estimate, by the order of magnitude, the limit charge which the crystal may have:

$$q \approx l^2\sqrt{2k}$$

At $l = 10^{-3}$ cm, $k = 2.8 \cdot 10^3$ erg/cm^3, it is easy to find q = 0.2 CGSE. A drop with the radius I, according to the Rayleigh criterion, can have the charge

$$Q \lesssim \sqrt{16\pi\sigma l^3}$$

We can easily obtain $Q \lesssim 2 \cdot 10^{-3}$ CGSE from the above expression at $\sigma = 75.6$ dyn/cm, i.e., it is on three orders of magnitude less than on a crystal of the same dimensions.

7. Conclusion

It is possible to assert, on the basis of what has been said, that both BL and SEF are forms of thunderstorm activity and ought to be studied in combination. They have much in common in appearance and in appearance conditions. Both are strictly attached to thunderstorm conditions. And though we still know little about the appearance mechanism and structure laws of BL (in spite of a great number of publications), those of SEF happen to have been revealed more easily. It seems that the analysis of the appearance conditions of SEF may be used as a source of information for BL appearance conditions and structure. This is probable, since eyewitnesses often report simultaneous appearances of BL and SEF. In the conclusion of the article we present one such testimony made by V. Y. Ilyinov:

On the 16 of August, 1977, we [a group of mountaineers] were climbing the Albrus. At a height of 3,900–4,000 m we came into a zone of increased electricity. Immediately, sparks started falling off from a raised ice-axe. We had to either carry on climbing or come down. We decided to go up. As soon as we approached a house for a rest (at a height of 4,200 m), a storm broke and went on for three days. A wind of 20–30 m/s was blowing with gusts up to 50 m/s. About two o'clock at night, I came out to the porch. There was total darkness above at about —4,800 meters. Just under me there was a dilapidated building. I could see still tongues of light-blue flame on every point of steel framework which protruded from the ruins. The flame was of various sizes. The higher was the point, the larger was a tongue of flame on it. Still lower at a height of 4,000 to 4,100 m, lightning was flashing. Orange balls of the size of a soccer ball were flying by the wind on the background of black clouds. There were about 10 of them. They were moving without system and burst with hissing which could be heard in spite of the wailing of the wind.

References

Brand, W. (1923). Der Kugelblitz. Hamburg: Henri Grand.

Engle, A. H. (1955). ***Ionized cases.*** Oxford: Clarendon Press.

English, W. N. (1948). Corona from water drop. ***Phys. Rev. 74***(2), 179–189.

Flammarion, K. (1873). ***The atmosphere.*** New York: Harper and Bros.

Griffiths, R. V., & Latham, J. (1974). A new method for the measurement of the electrical conductivity of ice. ***J. Meth. Sci. Japan.*** 52 (2), 238–242.

Grigor'ev, A. I. (1985a). St. Elmo's fire: ***Man and the elements*** [in Russian] Leningrad ÷ Gidrometeoizdat. p. 51–53.

Grigor'ev, A. I. (1985b). Some features of the corona discharge from the surface of snow and ice. ***Sov. Tech. Phys. Lett. 11***(8): 415–417.

Grigor'ev, A. I. (1985c). Mechanism for instability in a charged conducting droplet. ***Sov. Phys. Tech. Phys. 30***(7), 736–739.

Grigor'ev, A. I., & Grigor'eva I. D. (1986). St. Elmo's fire: Statistical processing of the observation data under natural conditions, experimental and theoretical investigations. ***Abstracts of the 3 All-Union Symposium on Atmospheric Electricity*** [in Russian] Tartu, September 28–31, 1986, p. 160.

Grigor'ev, A. I., & Sinkevich, O. A. (1984). A mechanism for St. Elmo's fire. ***Sov. Phys. Tech. Phys. 29***(7): 735–739.

Grigor'ev, A. I., & Sinkevich, O. A. (1985). Mechanism of development of the instability of a liquid drop in an electric field. ***Fluid Dynamics.*** 20 (6), 341–346.

Grigor'ev, A. I., & Shiryaeva, S. O. (1988). The parameters of electrostatic atomization. *Fluid Dynamics. 23* (2) 161–168.

Grigor'ev, A. I., Grigor'eva, I. D., & Shiryaeva, S. O. (1988). Statistical analysis of the ball lightning properties. *Science of Ball Lightning (Fire ball). Tokyo, Japan, 4–6 July 1988. Singapore. World Scientific. 1988.* pp. 88–134.

Grigor'ev, A. I., & Shiryaeva, S. O. (1989). Disintegration laws of a heavily charged drop [in Russian] *Zh. Tekh. Fiz. 59* (11), 119–121.

Grigor'ev, A. I., Zemskov, A. A., & Shiryaeva, S. O. (1988). Origin of the neutral droplets in the ion beams from liquid-metal ion sources. *Sov. Tech. Phys. Lett. 14* (9), 713–714.

Kalechits, V. I., Nahutin, I. Y., & Poluektov, P. P. (1982). On a possible mechanism for radio radiation of convective clouds [in Russian] *Dokl. Akad. Nauk SSSR 262* (6), 1344–1347.

Landau, L. D., & Lifshitz, E. M. (1984). *Electrodynamics of continuous media.* Oxford: Pergamon Press.

Lozanskii, E. D., & Firsov, O. B. (1975). Theory of sparks. [in Russian] Moscow: Atomizdat.

Matveev, L. T., (1984). *Course in general meteorology. Physics of the atmosphere.* [in Russian]. Leningrad: Gidrometeoizdat.

National Academy of Sciences. (1986). *Studies in geophysics. The Earth's electrical environment.* Washington: National Academy Press.

Olsen, R. G. (1983). Radio noise fields generated by corona streamers on a power line. *Radio Sci. 18* (3), 399–408.

Powell, J. R., & Finkelstein, D. (1969). Structure of ball lightning. *Advances in Geophys. 13,* 141.

Powell, J. R., & Finkelstein, D. (1970). Ball lightning. *American Scientist, 58,* 262.

Rayleigh, Lord (1882). On the equilibrium of liquid conducting masses charged with electricity. *Phyl. Mag., 14,* 184–186.

Tonks, L. (1935). A theory of liquid surface rupture by a uniform electric field. *Phys. Rev. 48,* 562–568.

Voitsekhovskii, B. B. (1982). St. Elmo's fire and luminescence on objects in a cloud of electrical charged water droplets. *Sov. Phys. Dokl. 27,* 54–57.

Zeleny, J. (1914). The electrical discharge from liquid points and hydrostatic method of measuring the electric intensity at their surface. *Phys. Rev. 3* (2), 69–91.

Zolotoi, N. B., Karpov, G. V., & Skyrat, V. Y. (1988). On the mechanisms for formation of ions and ion clusters from charged drops. *Zh. Tekh. Fiz. 58* (2), 307–315.